


RESEARCH PAPER

A sphingosine-1-phosphate receptor type 1 agonist, ASP4058, suppresses intracranial aneurysm through promoting endothelial integrity and blocking macrophage transmigration

Correspondence Shuh Narumiya, Center for Innovation in Immunoregulation Technology and Therapeutics, Kyoto University Graduate School of Medicine, Yoshida-Konoe-cho, Sakyo-ku, Kyoto, Kyoto, 606-8501, Japan. E-mail: snaru@mfour.med.kyoto-u.ac.jp

Received 22 November 2016; **Revised** 28 March 2017; **Accepted** 29 March 2017

Rie Yamamoto^{1,2} , Tomohiro Aoki¹, Hirokazu Koseki^{1,3}, Miyuki Fukuda¹, Jun Hirose^{1,2}, Keiichi Tsuji⁴, Katsumi Takizawa⁵, Shinichiro Nakamura⁶, Haruka Miyata^{1,4}, Nozomu Hamakawa², Hidetoshi Kasuya³, Kazuhiko Nozaki⁴, Yoshitaka Hirayama^{1,2}, Ichiro Aramori^{1,2} and Shuh Narumiya¹

¹Center for Innovation in Immunoregulation Technology and Therapeutics, Kyoto University Graduate School of Medicine, Kyoto, Japan, ²Tsukuba Research Center, Drug Discovery Research, Astellas Pharma Inc., Ibaraki, Japan, ³Department of Neurosurgery, Tokyo Women's Medical University Medical Center East, Tokyo, Japan, ⁴Department of Neurosurgery, Shiga University of Medical Science, Shiga, Japan, ⁵Department of Neurosurgery, Japanese Red Cross Asahikawa Hospital, Hokkaido, Japan, and ⁶Department of Stem Cells and Human Disease Models, Research Center for Animal Life Science, Shiga University of Medical Science, Shiga, Japan

BACKGROUND AND PURPOSE

Intracranial aneurysm (IA), common in the general public, causes lethal subarachnoid haemorrhage on rupture. It is, therefore, of utmost importance to prevent the IA from rupturing. However, there is currently no medical treatment. Recent studies suggest that IA is the result of chronic inflammation in the arterial wall caused by endothelial dysfunction and infiltrating macrophages. The sphingosine-1-phosphate receptor type 1 (S1P₁ receptor) is present on the endothelium and promotes its barrier function. Here we have tested the potential of an S1P₁ agonist, ASP4058, to prevent IA in an animal model.

EXPERIMENTAL APPROACH

The effects of a selective S1P₁ agonist, ASP4058, on endothelial permeability and migration of macrophages across an endothelial cell monolayer were tested *in vitro* using a Transwell system, and its effects on the size of IAs were evaluated in a rat model of IA.

KEY RESULTS

S1P₁ receptor was expressed in endothelial cells of human IA lesions and control arterial walls. ASP4058 significantly reduced FITC-dextran leakage through an endothelial monolayer and suppressed the migration of macrophages across the monolayer *in vitro*. Oral administration of ASP4058 reduced the vascular permeability, macrophage infiltration and size of the IAs by acting as an S1P₁ agonist in the rat model. This effect was mimicked by another two structurally-unrelated S1P₁ agonists.

CONCLUSION AND IMPLICATIONS

A selective S1P₁ agonist is a strong drug candidate for IA treatment as it promotes the endothelial cell barrier and suppresses the trans-endothelial migration of macrophages in IA lesions.

Abbreviations

ACA, anterior cerebral artery; BAPN, 3-aminopropionitrile; geoMFI, geometric mean fluorescence intensity; HCtAEC, human carotid artery endothelial cells; IA, intracranial aneurysm; MC, methylcellulose; OA, olfactory artery; SMA, α -smooth muscle actin; S1P, sphingosine-1-phosphate; WSS, wall shear stress

Introduction

Sphingosine-1-phosphate (S1P) is a bioactive lipid exerting its action through five GPCR subtypes, **S1P₁**, **S1P₂**, **S1P₃**, **S1P₄** and **S1P₅** (Blaho and Hla, 2014). The most well-known physiological function of S1P receptors is that of the S1P₁ receptor in lymphocyte trafficking. In this process, S1P₁ receptors on T lymphocytes respond to the S1P gradient between secondary lymphoid organs and blood, and promote the release of lymphocytes from the lymphoid organs to the blood stream. An S1P₁ agonist administered at active doses causes the internalization of S1P₁ receptors on lymphocytes, resulting in impaired lymphocyte release and a decrease in peripheral lymphocytes count, and thereby functions as an immunosuppressant (Brinkmann *et al.*, 2004; Matloubian *et al.*, 2004). A notable example is **fingolimod (FTY720)**, which is clinically used for multiple sclerosis (Brinkmann, 2009; Brinkmann *et al.*, 2010). The role of S1P-S1P₁ receptor signalling in the vascular system is physiologically important, as well as in the immune system; this includes the promotion and maintenance of endothelial barrier function (Schuchardt *et al.*, 2011). Stimulation of S1P₁ receptors on endothelial cells activates Rac, leading to the formation of the cortical actin ring by translocating cortactin to the cell periphery (Marsolais and Rosen, 2009; Xiong and Hla, 2014). This cytoskeletal rearrangement facilitates the assembly of tight and adherens junction components to strengthen endothelial barrier function (Lee *et al.*, 1999; Lee *et al.*, 2006). Importantly, disruption of the endothelial barrier function underlies the pathogenesis of not only various vascular diseases but also neurodegenerative diseases and cancer (Rodrigues and Granger, 2015). Thus, the S1P₁ receptor on endothelial cells could be a therapeutic target of these diseases.

Intracranial aneurysm (IA) is the balloon-like bulging at bifurcation sites of the intracranial artery histopathologically characterized by degenerative changes and inflammatory infiltrates in arterial walls. IA is fairly common in the general public with a prevalence of 3 to 5% and it is a major cause of subarachnoid haemorrhage (Wardlaw and White, 2000; Wiebers *et al.*, 2002; van Gijn *et al.*, 2007), which ends in a poor prognosis. About a half of the affected individuals die and survivors suffer from a lifetime disability (van Gijn *et al.*, 2007). Therefore, it is socially important to prevent the IA from rupturing. Nonetheless, there is no medical treatment for IA, and IA patients can only be treated with surgical manipulations such as microsurgical clipping and endovascular coiling. Since surgical manipulations have an intrinsic risk of complications, IAs prone-to rupture, such as large ones or those with an irregular shape, are selected for surgery (van Gijn *et al.*, 2007; Greving *et al.*, 2014; Etminan *et al.*, 2015), leaving many IA cases without treatment. Given the high prevalence of IAs in the general public and poor prognosis of subarachnoid haemorrhage, there is an urgent need to develop a drug therapy for IA.

IA can be produced experimentally in animals and this experimentally-induced IA lesion shares many features in common with human IA, such as the degeneration of the media and macrophage infiltration. Evidence has accumulated from these animal experiments to suggest that IA is a disease caused by chronic inflammation of intracranial

arteries in which infiltrated macrophages play a crucial role (Aoki and Nishimura, 2010; Aoki and Narumiya, 2012; Fukuda and Aoki, 2015). Indeed, some experimental conditions that prevent macrophage recruitment and accumulation in the IA wall, such as pharmacological depletion of macrophages by clodronate liposome and genetic deletion of **CCL2 (MCP-1)**, a major chemoattractant for recruiting macrophages to affected sites, remarkably and significantly suppressed the incidence and size of IAs in a model of IA (Aoki *et al.*, 2009; Kanematsu *et al.*, 2011). Hence, inhibition of macrophage recruitment in lesions or sites prone to IA formation could be a therapeutic approach for treating IAs or preventing their *de novo* formation. Because of the lack of vasa vasorum in the adventitia of intracranial arteries, macrophages present in IA walls are presumably derived from monocytes in the blood stream, which adhere to endothelial cells activated at the site of prospective IA lesion and infiltrate into arterial walls across the endothelium. IA occurs at the bifurcation sites of the intracranial artery, where computational fluid dynamic analyses in both human IAs and those in animal models have revealed the presence of a high wall shear stress (WSS) (Dolan *et al.*, 2013; Turjman *et al.*, 2014). As endothelial cells in culture respond to WSS and change their gene expression profiles, including the induction of **COX-2 in vitro** (Ohura *et al.*, 2003; Aoki *et al.*, 2011), high WSS is likely to activate endothelial cells at bifurcation sites, which then trigger inflammation in arterial walls thereby promoting IA pathology (Turjman *et al.*, 2014; Fukuda and Aoki, 2015). In support of this notion, in a rodent IA model, activation of endothelial cells (as indicated by NF- κ B activation, MCP-1, **VCAM-1** and COX-2 induction) was demonstrated to occur at sites of IA formation (Aoki *et al.*, 2007; 2011 Aoki and Nishimura, 2010). In addition, a defect in the lining of endothelial cells was observed in human IAs (Frosen *et al.*, 2004), suggesting the presence of endothelial damage at sites of IA formation and rupture through aberrant flow conditions. Consistently, endothelial cell damage was observed in the very early stage of IA induction in rats and the expressions of genes for tight junction-components such as occludin and ZO-1 were reduced at these sites (Tada *et al.*, 2010), which presumably facilitates the trans-endothelial infiltration of macrophages. Based on these findings, compounds that strengthen barrier function including the tight junction between endothelial cells or close the already loose barrier could be drug candidates for IA treatment. Here, we have examined the potential of S1P₁ agonists as endothelium-modulating drugs for IA treatment.

Methods

Study approval

The use of human IA specimens and control arterial walls in the present study was approved by the ethics committee at Kyoto University Graduate School and Faculty of Medicine (#E2540 and #R0601), ethical committee of Japanese Red Cross Asahikawa Hospital (#201441-2) and Astellas Research Ethics Committee (#150011-2). Patients with unruptured IAs were informed of the purpose, benefit and demerit of the study and written informed consent was then obtained

from every participant on a voluntary basis before harvesting specimens.

All of the following experiments including animal care and use complied with the National Institutes of Health Guide for the Care and Use of Laboratory Animals and were approved by the Animal Research Committee of Kyoto University Graduate School of Medicine (MedKyo12037, 13558, 14073, 15057 and 16537).

Experiments on non-human primates was approved by The Animal Care and Use Committee at Shiga University of Medical Science (2013-10-2HHHH) and Institutional Animal Care and Use Committee of Astellas Pharma (D-T14090-01, D-T15382-01). All of the animal studies were conducted with a careful consideration of the 3Rs (replacement, reduction and refinement). Animal studies are reported in compliance with the ARRIVE guidelines (Kilkenny *et al.*, 2010; McGrath & Lilley, 2015).

Cell culture

Primary cultures of human carotid artery endothelial cells (HCtAEC) were used as an alternative to ones from intracranial arteries, which were not available. HCtAEC (Lot no. 2366) was purchased from Cell Applications (San Diego, CA) and was cultured in MesoEndo Cell Growth Medium (Cell Applications). THP-1, a cell line derived from acute monocytic leukaemia patient, was used as an alternative to peripheral monocytes. THP-1 cells were from ATCC (Manassas, VA) and cultured in RPMI 1640 medium (Nacalai Tesque, Kyoto, Japan) supplemented with 10% FBS (GE Healthcare Life Sciences, Marlborough, MA), 50 µg·mL⁻¹ streptomycin and 50 U·mL⁻¹ penicillin (Thermo Fisher Scientific, Carlsbad, CA). CHO-K1 cells overexpressing human S1P₁ receptors (hS1P₁) previously established by Yamamoto *et al.* (2014) were cultured in Ham's F12 medium supplemented with 10% FBS (GE Healthcare), 50 µg·mL⁻¹ streptomycin and 50 U·mL⁻¹ penicillin (Thermo Fisher Scientific) and 1 mg·mL⁻¹ G418 sulfate (Nacalai Tesque). All cells were maintained at 37°C in 5% CO₂.

PCR

Total RNA was prepared from HCtAECs using an RNeasy Plus Mini Kit (QIAGEN, Hilden, Germany), and transcribed to cDNA using a High-Capacity cDNA Reverse Transcription Kit (Life Technologies Corporation, CA). Conventional RT-PCR was then carried out using a KOD FX (Toyobo, Osaka, Japan) and amplified products were separated by agarose-gel electrophoresis. Primer sets used are forward; 5'-agaagtgcacactcacttg-3' and reverse 5'-agctcctaaagggttcatttg-3' for S1P₁ receptor, forward 5'-gaggtctgagaatgaggaatgg-3' and reverse 5'-cactgtctctgaggagctagagg-3' for S1P₂ receptor, forward 5'-agaagatcccattctgaagtgc-3' and reverse 5'-cccaagcagaagtaatacaagc-3' for S1P₃ receptor, forward 5'-atcatcagcaccgtcttcagc-3' and reverse 5'-ctctactccaagcgtacatcc-3' for S1P₄ receptor, forward 5'-gagctataattgtgccattgc-3' and reverse 5'-atttgactctgggagactcagc-3' for S1P₅ receptor.

cAMP assay

HCtAECs were seeded at 2 × 10⁴ cells per well in 96 well plates and incubated overnight. ASP4058 was dissolved in DMSO (Nacalai Tesque) and then diluted to a working concentration with stimulation buffer composed of 5 mM HEPES (pH 7.5),

0.1% fatty acid-free BSA (Sigma-Aldrich, St. Louis, MO), and 0.5 mM IBMX in HBSS (pH 7.2). HCtAECs were treated with 1 µM **forskolin** (Sigma-Aldrich) in the presence of ASP4058 for 20 min at 37°C and then lysed with lysis buffer (50 mM HEPES, 10 mM CaCl₂, 0.35% Triton X-100). **cAMP** concentration in cell lysates was examined using a LANCE cAMP 384 kit (PerkinElmer Life and Analytical Sciences, Shelton, CT) according to the manufacturer's instructions. Each experiment was performed in duplicate to ensure the reliability of single values.

S1P₁ receptor internalization assay

HCtAECs were seeded at 10⁵ cells per well in a 96 well plate and incubated overnight. ASP4058 dissolved in DMSO was diluted with endothelial cell serum-free defined medium (Cell Applications). Cells were treated with the indicated concentration of ASP4058 (as shown in the Figures, Legends or the Results) for 1 h at 37°C. After being washed with ice cold PBS, cells were harvested using an Accutase (Nacalai Tesque). After being washed with FACS buffer (PBS supplemented with 0.5% fatty acid free BSA and 0.1% sodium azide), cells were stained with mouse anti-S1P₁ antibody (#MAB2016, R&D systems, Minneapolis, MN) for 30 min on ice followed by the incubation with anti-mouse IgG conjugated with PE (#405307, Biolegend, San Diego, CA). Purified mouse IgG_{2b} (#400302, Biolegend) was used as an isotype control. Cells were then analysed using an LSRFortessa (BD biosciences, San Jose, CA) and a FlowJo software (FlowJo, Ashland, OR). Dead cells were stained with either 7-aminoactinomycin D (Sigma-Aldrich) or a SYTOX Blue dead cell stain (Thermo Fisher Scientific) and gated out. The expression level of surface S1P₁ receptors was determined as geometric mean fluorescence intensity (geoMFI) of PE-positive cells after subtracting that of isotype control (δ geoMFI). δ geoMFI of ASP4058-treated cells was normalized to that of vehicle-treated control to control for the inter-experimental technical variability and expressed as a percentage of control.

Permeability assay

HCtAECs were seeded at 10⁵ cells per well in a Transwell insert coated with collagen (diameter: 6.5 mm, pore size: 0.4 µm) (#3495, Corning, Tewksbury, MA) and cultured overnight in MesoEndo Growth Medium (Cell Applications). The medium was replaced with endothelial cell serum-free defined medium (Cell Applications), and the cells were further cultured overnight. ASP4058 dissolved in DMSO was diluted with serum-free medium. Vehicle (0.1% DMSO) or ASP4058 was then added to both the upper and the lower compartments of a Transwell. After 1 h, 250 µg·mL⁻¹ of FITC-dextran (2000 kDa; Sigma-Aldrich) was added to the upper compartment, and the amount of FITC-dextran diffused into the lower compartment for 1 h was determined by measuring the fluorescence intensity of the medium in the lower compartment using a FlexStation 3 microplate reader (Molecular Devices, Sunnyvale, CA) at excitation wavelength of 490 nm and emission wavelength of 520 nm. In some experiments, cells were pretreated with various concentration of an S1P₁ antagonist, TASP0277308 for 1 h, or a Rac inhibitor, EHop-016 (Sigma-Aldrich) for 30 min, followed by addition of ASP4058 (100 nM). Each experiment was

performed in duplicate to ensure the reliability of single values at 37°C.

Trans-endothelial migration assay

HCtAECs were seeded at 10^5 cells per well in a Transwell insert (diameter: 6.5 mm, pore size: 5.0 μm) (#3421, Corning) and cultured overnight in MesoEndo Growth Medium (Cell Applications). ASP4058 dissolved in DMSO was diluted with endothelial cell serum-free defined medium (Cell Applications). Vehicle (0.1% DMSO) or ASP4058 was then added to both the upper and the lower compartments. Simultaneously, THP-1 cells, used as an alternative to peripheral monocytes, (5×10^5 cells per well) and MCP-1 (100 $\text{ng}\cdot\text{mL}^{-1}$) were added to the upper and the lower compartment respectively. After 3 h incubation at 37°C, the number of migrated cells was determined using a Cell Titer Glo Luminescent cell viability assay (Promega, Madison, WI) according to the manufacturer's instructions. In some experiments, various concentrations of TASP0277308 were added simultaneously with ASP4058 (100 nM). Each experiment was performed in duplicate to ensure the reliability of single values.

Chemotaxis assay

The chemotaxis of THP-1 cells was measured using Transwell inserts (diameter: 6.5 mm, pore size: 5.0 μm) (#3421, Corning). ASP4058 dissolved in DMSO was diluted with RPMI 1640 medium (Nacalai Tesque) supplemented with 0.1% fatty acid free BSA (Sigma-Aldrich). Vehicle (0.1% DMSO) or ASP4058 was then added to both the upper and the lower compartments. Simultaneously, THP-1 cells (5×10^5 cells per well) and MCP-1 (10 $\text{ng}\cdot\text{mL}^{-1}$) were added to the upper and the lower compartment respectively. After 3 h incubation at 37°C, the number of migrated cells was determined using a Cell Titer Glo Luminescent cell viability assay (Promega). Each experiment was performed in duplicate to ensure the reliability of single values.

Rodent IA models and histological analysis of induced IAs

Sprague–Dawley rats were purchased from Japan SLC (Shizuoka, Japan) and were housed in sterile cages (maximum three rats per cage) in an individually ventilated rack system under specific-pathogen free conditions and maintained with standard housing and husbandry conditions under a 14 h light and 10 h dark cycle and had a free access to food and water. To induce IA, male rats, 7-weeks-old, were subjected to ligation of left carotid artery and left renal artery under general anaesthesia, induced by i.p. injection of pentobarbital sodium (50 $\text{mg}\cdot\text{kg}^{-1}$), to increase haemodynamic stress at bifurcation sites contralateral to the carotid ligation. IAs induced in this model share several histological and functional characteristics with human IAs (Aoki, 2015), and this has been used for decades as one of the major animal models of IA to examine mechanisms underlying its pathogenesis (Hashimoto *et al.*, 1978; Aoki and Nishimura, 2011). After full recovery from anaesthesia, animals were randomly divided into groups by an independent investigator and fed a high-salt diet containing 8% sodium chloride beginning immediately after surgical manipulation to induce systemic hypertension by salt-overloading. In some

experiments, as indicated in the Figure legends, 0.12% 3-aminopropionitrile (BAPN) (Tokyo Chemical Industry, Tokyo, Japan), an inhibitor of lysyl oxidase, which catalyses the cross-linking of collagen and elastin, was added in the chow to weaken the extracellular matrix and facilitate IA formation. IA induction at the bifurcation site of the right anterior cerebral artery (ACA)-olfactory artery (OA), a contralateral side of carotid ligation, was assessed at different times. Systemic blood pressure was measured by the tail-cuff method (BP-98A, Softron, Tokyo, Japan) without any anaesthesia and its value was calculated as a mean of at least three measurements. For histological analyses, animals were deeply anaesthetised by an i.p. injection of a lethal dose of pentobarbital sodium and transcardially perfused with 4% paraformaldehyde. The right ACA-OA bifurcation including the IA lesion was dissected out and serial frozen sections at 5 μm thickness were prepared. IA formation at this bifurcation was examined after Elastica van Gieson staining. IA was defined as a lesion with a disrupted internal elastic lamina, and its size was calculated as an average value of transverse diameter between the edge of disrupted elastic lamina and maximum perpendicular length (height). The thickness of the medial smooth muscle cell layer was measured at the thinnest portion of IA walls immunostained by the smooth muscle cell marker, α -smooth muscle actin (SMA). Histological analyses were performed by independent investigators who were blinded to group assignment. Moribund animals were killed by CO_2 inhalation according to humane endpoints. A total of 232 animals were surgically manipulated, but of these 15 animals (6.5%) were excluded because they died during the experimental period. We did not exclude any animals from the analyses except for ones that died.

Administration of ASP4058 or other compounds to the rat model of IAs

Rats subjected to the aneurysm induction were randomized and administered ASP4058 or other compounds suspended in the vehicle p.o. The vehicle for all compounds except for TASP0277308 was 0.5% methylcellulose solution (MC), and for TASP0277308, the vehicle was 5% arabic gum solution. The dose and administration period of each compound are indicated in the Figure legends or the Results section.

Immunohistochemistry

IA specimen was harvested as described above and slices of 5 μm thickness were prepared. After being blocked with 3% donkey or goat serum (Jackson ImmunoResearch, Baltimore, MD), the slices were incubated with primary antibodies followed by incubation with secondary antibodies conjugated with fluorescent dye (Invitrogen, Waltham, MA). In some experiments, DyLight488-conjugated *Lycopersicon esculentum* Lectin (Vector Laboratories, Burlingame, CA) was used instead of an antibody to visualize endothelial cells. Finally, immunofluorescence images were acquired on a confocal fluorescence microscope system (LSM-710, Carl Zeiss Microscopy GmBH, Gottingen, Germany).

Primary antibodies used were; mouse monoclonal anti-smooth muscle α actin antibody (#MS113, Thermo Fisher Scientific, Waltham, MA), rat monoclonal anti-F4/80 antibody

(#ab16911, Abcam, Cambridge, UK), goat polyclonal anti-MCP-1 antibody (#sc-1785, Santa Cruz Biotechnology, Dallas, TX), rabbit polyclonal anti-S1P1 antibody (#sc-25489, Santa Cruz Biotechnology).

Transmission electron microscopy

At 5 days after the aneurysm induction, rats were killed as described previously. Dissected IA preparations were fixed in 4% paraformaldehyde in 0.1 M sodium phosphate buffer (pH 7.4). Fixed specimens were then stained with 1% osmium tetroxide (Wako Pure Chemical Industries, Osaka, Japan) in 0.1 M sodium phosphate buffer (pH 7.4) for 1 h at room temperature. After dehydration in a series of graded ethanol solutions and replacement by propylene oxide (Nacalai Tesque), specimens were embedded in epoxy resin (Nacalai Tesque) overnight followed by the polymerization for 72 h. Ultrathin sections were prepared and images were obtained using an H-7650 Transmission Electron Microscope (Hitachi, Tokyo, Japan).

In vivo vascular permeability assay

Rats were subjected to the IA induction as described previously and administered ASP4058 or 0.5% MC as a vehicle, p.o., once a day from just after the surgical manipulation. On the seventh day after the induction, rats were deeply anaesthetised as described previously and the right common carotid artery was surgically exposed. Evans blue (45 mg·kg⁻¹, Wako Pure Chemical Industries) was injected intra-arterially after the proximal side of injection had been clamped with a micro serrefine (FST, Foster City, CA) followed by the perfusion with 4% paraformaldehyde. As a control, age-matched Sprague–Dawley rats were used. Frozen sections were prepared as described previously and fluorescence images of Evans blue (excitation; 620 nm per emission; 680 nm) were acquired on a confocal fluorescence microscope system. The Evans blue-stained area at ACA-OA bifurcation was calculated using Fiji (<http://fiji.sc/>). In brief, the images acquired were converted to binary images after colour threshold adjustment, and all the particles more than the size of 4 pixel square were picked up as positive signals to exclude non-specific signals.

Non-human primate model of IAs

Female *Macaca fascicularis* from Vietnam (imported by Keairi, Osaka, Japan), 11-years-old of age and 3.4 kg average body weight, were used in the present study. Animals were housed in a temperature- and humidity-controlled room under a 12 h light–dark cycle. To induce IAs, animals were underwent two-step surgical manipulations with a 2 week interval; the first was laparoscopic bilateral oophorectomy, and the second was ligation of left hilum of kidney and left carotid artery, under general anaesthesia with i.m. administration of ketamine hydrochloride (Daiichi Sankyo Inc., Tokyo, Japan, 5 mg·kg⁻¹) and xylazine hydrochloride (Bayer Inc., Osaka, Japan, 1 mg·kg⁻¹) and inhalation of isoflurane (InterVet Inc., Tokyo, Japan). Bilateral oophorectomy was applied to this model to enhance the incidence of IA, as described previously (Jamous *et al.*, 2005). Animals were injected i.m. with analgesia (Flunixin Meglumine, 1 mg·kg⁻¹; Nagase medicals, Hyogo, Japan) and antibiotics (Mycillin Sol, 0.1 mL·kg⁻¹; Meiji Seika, Tokyo, Japan) after surgical

manipulations. At 1 and 2 weeks after surgical manipulations, treatment with sodium chloride (1% in drinking water) and BAPN (0.2%) was started respectively. Animals were randomly assigned to each group by an independent investigator and ASP4058 (0.1 mg·kg⁻¹) or vehicle (0.5% MC) was administered once daily from the day of the second surgical manipulations and repeated throughout the entire experimental period for 52 weeks.

After the animals had been killed by an i.v. injection of sodium pentobarbital (Kyoritsu Seiyaku, Tokyo, Japan), the brain with the ring of Willis was harvested and fixed in formalin solution for at least 1 week. After fixation, each bifurcation site of intracranial arteries was dissected and embedded in paraffin. Slices, 4 µm thick, were then prepared for histopathological analyses. IA formation at each bifurcation was assessed after visualization of internal elastic lamina by Elastica van Gieson Staining. The assessment was performed by independent investigators who were blinded to group allocation. IA is defined as a lesion with disrupted internal elastic lamina. No animals met the humane endpoints before the end of the experiment.

Plasma concentration of ASP4058

Blood samples were collected from rats and non-human primates that had received ASP4058. Plasma was then separated by centrifugation and stored at –20°C or lower. Samples were prepared using protein precipitation, and plasma concentrations were determined using HPLC–tandem mass spectrometry.

Human specimens and immunohistochemistry

Human IA samples and control arterial walls (superficial temporal artery or middle meningeal artery) were dissected during microsurgical clipping of unruptured IAs with the written informed consent of the patients. Dissected specimens were fixed in formalin solution and embedded in paraffin. Then 4 µm thick slices were prepared for immunohistochemical analysis. Immunohistochemistry was carried out as described before after deparaffinization. Mouse monoclonal anti-human CD31 antibody (#M0823, Dako, Glostrup, Denmark) and rabbit polyclonal anti-S1P1 antibody (#sc-25489, Santa Cruz Biotechnology) were used as primary antibodies, and secondary antibodies conjugated with fluorescent dye (Invitrogen) were used to visualize the labelled cells. Cy3-conjugated mouse monoclonal anti-smooth muscle α actin antibody (#C6198, Sigma-Aldrich) was used to visualize smooth muscle cells. Finally, immunofluorescence images were acquired on a confocal fluorescence microscope system (LSM-710, Carl Zeiss Microscopy GmBH, Gottingen, Germany).

Data and statistical analysis

Data except for IC₅₀ values are shown as mean ± SEM; IC₅₀ values are represented as the geometric mean and 95% confidence interval. To determine IC₅₀ values, concentrations of an investigational compound were log transformed to create a sigmoidal curve and a four parameter concentration–response curve fitting model was used. Statistical comparisons between two groups were made using Student's unpaired *t*-test. Statistical comparisons among more than two groups were conducted using Dunnett's multiple comparison test. In the S1P₁ receptor internalization assay and *in vivo* vascular

permeability assay, Mann–Whitney *U*-test was used for statistical comparison between two groups, and Steel's multiple comparison test for comparison among more than two groups. A *P* value smaller than 0.05 was defined as statistically significant. All statistical analyses except for the Steel test were performed using a GraphPad Prism 5 (GraphPad Software, La Jolla, CA). The Steel test was performed using a JMP Pro 12 (SAS, Cary, NC). The data and statistical analysis comply with the recommendations on experimental design and analysis in pharmacology (Curtis *et al.*, 2015).

Compounds

ASP4058 hydrochloride (5-[5-[3-(trifluoromethyl)-4-[(2*S*)-1,1,1-trifluoropropan-2-yl]oxy]phenyl]-1,2,4-oxadiazol-3-yl]-1*H*-benzimidazole hydrochloride), KRP-203 (2-amino-2-[2-(4-[[3-(benzyloxy)phenyl]sulfanyl]-2-chlorophenyl)ethyl]propane-1,3-diol hydrochloride), **BAF312** (1-[4-[(1*E*)-*N*-[[4-cyclohexyl-3-(trifluoromethyl)benzyl]oxy]ethanimidoyl]-2-ethylbenzyl]azetidine-3-carboxylic acid), fingolimod hydrochloride (2-amino-2-[2-(4-*o*-cetylphenyl)ethyl]propane-1,3-diol hydrochloride) and TASP 0277308 (3,4-dichloro-*N*-[(1*R*)-1-[4-ethyl-5-[3-(4-methylpiperazin-1-yl)phenoxy]-4*H*-1,2,4-triazol-3-yl]ethyl]benzenesulfonamide) were synthesized at Astellas Pharma. EHOP-016 was purchased from Sigma-Aldrich (St. Louis, MO). All dosages and concentrations of these compounds were calculated as their respective free-base equivalent.

Nomenclature of targets and ligands

Key protein targets and ligands in this article are hyperlinked to corresponding entries in <http://www.guidetopharmacology.org>, the common portal for data from the IUPHAR/BPS Guide to PHARMACOLOGY (Southan *et al.*, 2016), and are permanently archived in the Concise Guide to PHARMACOLOGY 2015/16 (Alexander *et al.*, 2015).

Results

Expression of S1P₁ receptors in human IA walls

Since IA occurs at the bifurcation of intracranial artery, sites under high WSS, and endothelial activation in response to WSS is suggested to trigger IA, one strategy of IA treatment is to inhibit endothelial activation by pharmacological means. The S1P₁ receptor can be a good target, because stimulation of the S1P₁ receptor promotes endothelial integrity (Schuchardt *et al.*, 2011). To confirm the potential of this strategy, we first examined if the S1P₁ receptor is expressed in endothelial cells of human intracranial artery and whether this expression can be observed in IA lesions as well. We collected 5 IA lesions and two control arterial walls from patients with unruptured IA and immunostained sections from these specimens to examine the expression of S1P₁ receptors. In both of the control arterial walls, the S1P₁ receptor was detected as signals aligned along the luminal surface and those scattered in the media where α -SMA signals were similarly distributed and colocalized, and the former signals overlapped with those of CD31 (Figure 1A, Supporting Information Figure S1), indicating that the S1P₁ receptor is expressed in endothelial cells of the branches of carotid artery. In three out of five IA walls, S1P₁ receptor signals in

CD31⁺ cells were detected as well, but few signals were found in the media where SMA-positive signals were also absent (Figure 1B, Supporting Information Figure S1). These results suggest that S1P₁ receptors are present in endothelial cells in IA lesions, in which most smooth muscle cells are lost by degenerative changes. In the remaining two out of five IA lesions collected, endothelial cells were denuded and almost all vascular cells were lost. Consistent with the loss of endothelial cells, the expression of S1P₁ receptors in IA walls was not detectable any more in these IA lesions (Figure 1C, Supporting Information Figure S1).

ASP4058 promotes endothelial barrier function *in vitro* via S1P₁ receptors

To investigate how S1P₁ receptor signalling regulates endothelial barrier function and whether we can manipulate this function pharmacologically, we used primary cultures of endothelial cells (HCtAECs), and treated them with an S1P₁ agonist, ASP4058 (Yamamoto *et al.*, 2014). RT-PCR analysis revealed the expression of all S1P receptor subtypes except for S1P₅ in these cells (Figure 2A). ASP4058 stimulates S1P₁ and S1P₅ receptors with almost the same EC₅₀ values (7.4 and 7.5 nM, respectively), but its potency for other S1P receptor subtypes is at least 100 times less (Table 1) (Yamamoto *et al.*, 2014). ASP4058, therefore, selectively acts on S1P₁ receptors in HCtAECs. To characterize the action of ASP4058, we first examined its effect on forskolin-induced increases in intracellular cAMP, because S1P₁ is a Gi-coupled GPCR (Brinkmann, 2007), whose activation leads to a reduction in cAMP production *via* inhibition of adenylyl cyclase. HCtAECs were treated with forskolin in the presence of various concentrations of ASP4058, and the intracellular cAMP content was measured. As expected, ASP4058 concentration-dependently inhibited the cAMP accumulation in the cells, with an IC₅₀ value of 2.1 nM (95% CI: 0.81–5.7 nM) (Figure 2B). We next examined the potency of ASP4058 to induce S1P₁ receptor internalization, because S1P₁ receptors on the plasma membrane are rapidly internalized upon stimulation (Liu *et al.*, 1999) and it is essential to distinguish agonist activities from those of functional antagonism of each S1P₁ agonist. HCtAECs were incubated with various concentrations of ASP4058 for 1 h, and the expression of S1P₁ receptors on their surface was monitored by FACS analysis using anti-S1P₁ antibody. ASP4058 internalized S1P₁ receptors expressed on HCtAEC, and the S1P₁ receptor expression level on HCtAECs treated with 100 and 1000 nM ASP4058 was 86 ± 14 and 23 ± 4.3% of control respectively; the concentration required to internalize S1P₁ receptors was more than 50-fold higher than that needed to exert the above mentioned agonistic effect (Figure 2C, D).

We then examined the effect of ASP4058 on barrier function of endothelial cells. HCtAECs were cultured in a monolayer, and the permeability of FITC-labelled dextran (2000 kDa) across the monolayer was quantified in a Transwell system. Treatment of HCtAECs with ASP4058 decreased the leakage of FITC-dextran across the endothelial monolayer in a concentration-dependent manner and statistically

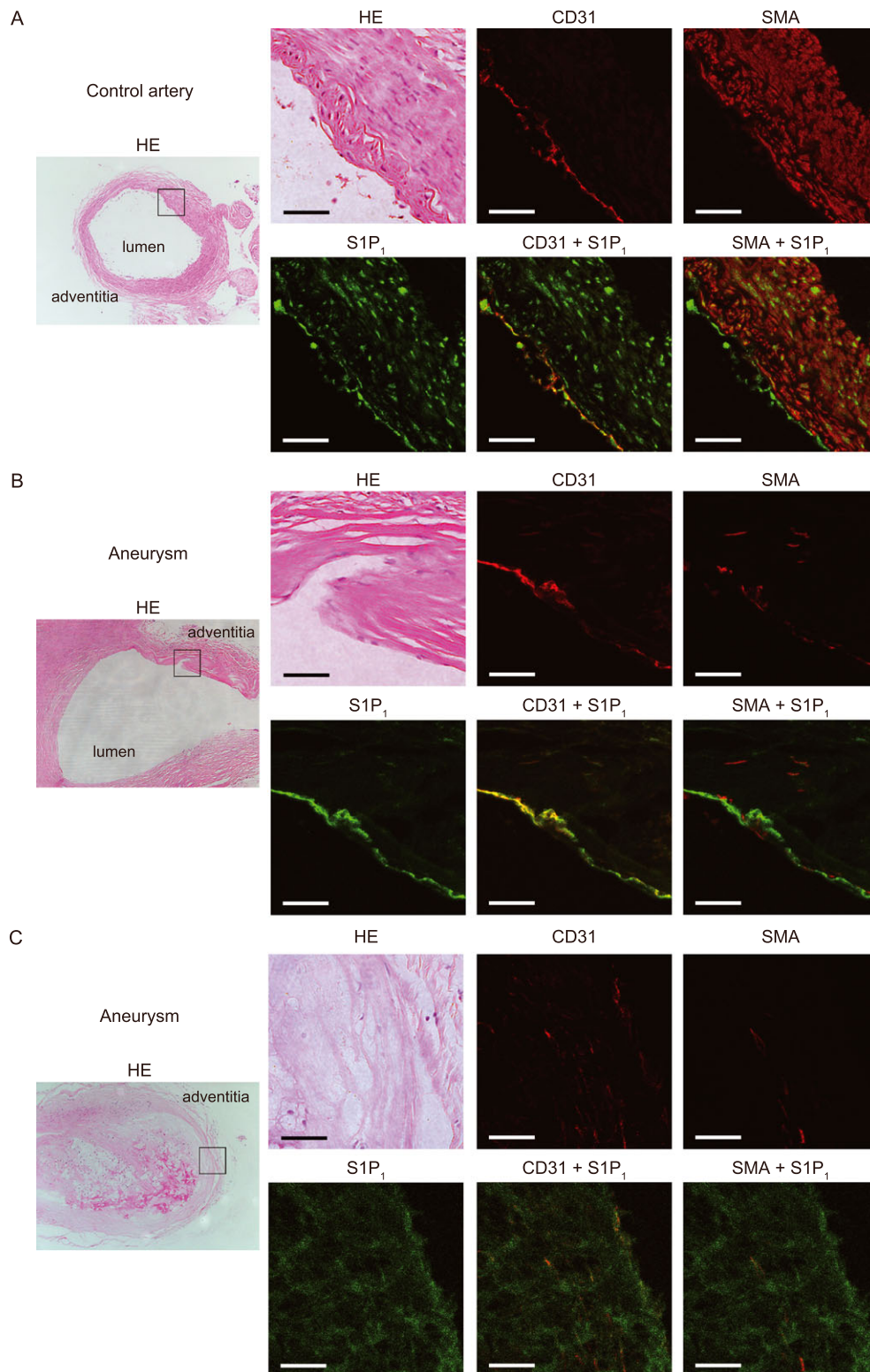


Figure 1

Expression of S1P₁ receptors in human control arterial wall (A) and IA lesion (B, C). Adjacent sections were prepared from branches of carotid artery or IA lesion of humans and immunostained for α -SMA, a medial smooth muscle marker, CD31, an endothelial cell marker and S1P₁ receptors. Merged images for CD31 and S1P₁ staining, SMA and S1P₁ staining and images with Haematoxylin–Eosin staining (HE) are also shown. Box in the left panels indicates the region magnified in the following panels. Bar, 50 μ m.

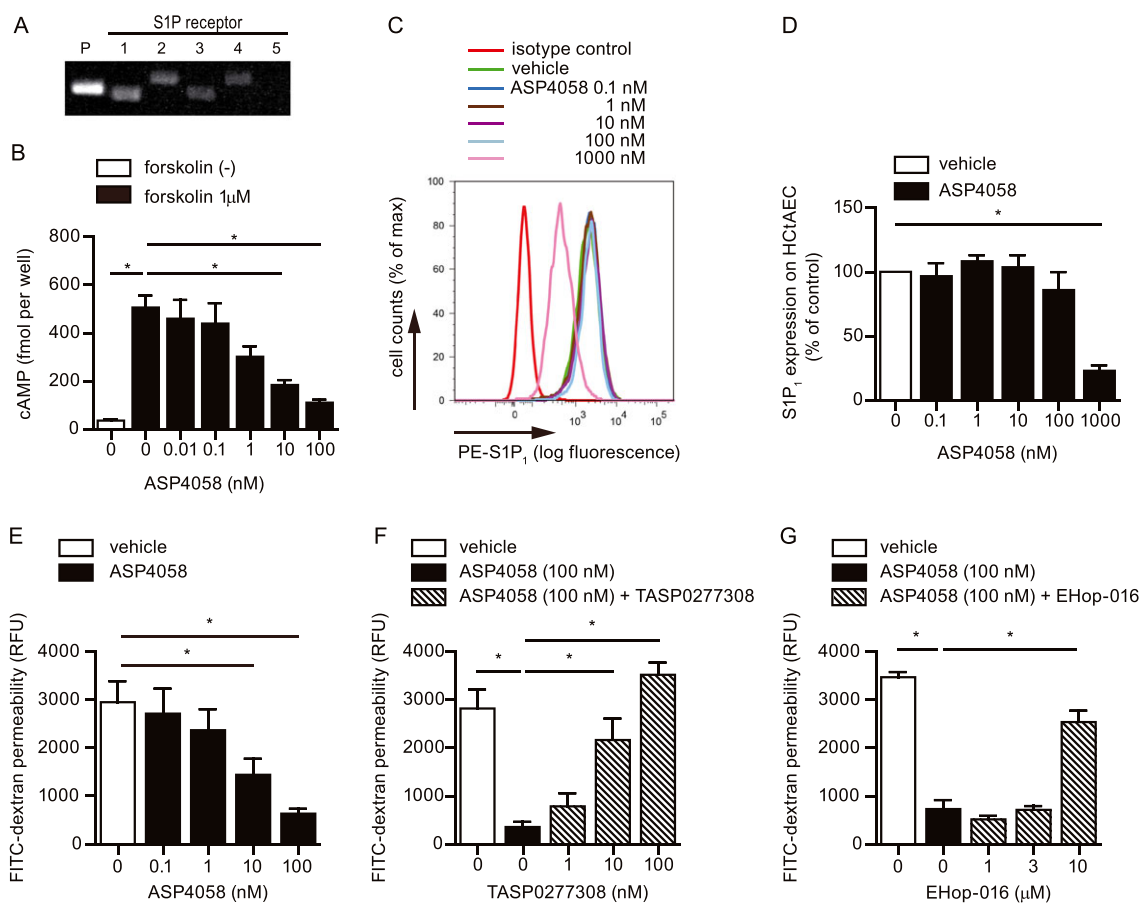


Figure 2

Inhibition of endothelial permeability by ASP4058 mediated by the S1P₁ receptor. (A) Expression of each S1P receptor subtype in primary culture of endothelial cells (HCTAECs). Primer set to detect β-actin mRNA served as a positive control (P). (B) Concentration-dependent inhibition of forskolin-induced cAMP accumulation in HCTAECs by ASP4058. HCTAECs were treated with 1 μM forskolin in the presence of the indicated concentrations of ASP4058, and cAMP accumulation was examined as described in the Methods. Data represent mean ± SEM ($n = 5$). * $P < 0.05$. (C, D) Effect of ASP4058 on surface expression of S1P₁ receptors in HCTAECs. HCTAECs were treated with the indicated concentrations of ASP4058 for 1 h, and the surface expression of S1P₁ receptors was examined by FACS. Representative histogram of FACS analysis for S1P₁ receptor is shown in (C) ($n = 5$). (D) The surface expression of S1P₁ receptors calculated as described in the Methods. Data represents mean ± SEM ($n = 5$). (E) Inhibition of endothelial permeability by ASP4058. HCTAECs cultured on a Transwell insert as a monolayer were treated with each concentration of ASP4058 for 1 h, and permeability across the monolayer was measured for 1 h by diffusion of 2000 kDa FITC-labelled dextran through the insert. RFU, relative fluorescent units. Data represent mean ± SEM ($n = 6$). * $P < 0.05$. (F, G) Effect of an S1P₁ receptor antagonist or a Rac inhibitor on the ASP4058-mediated inhibition of endothelial permeability. HCTAECs cultured on Transwell inserts were treated with 100 nM ASP4058 together with the indicated concentrations of an S1P₁ receptor antagonist, TASP0277308 (F), or a Rac inhibitor EHOp-016 (G), for 1 h, and the effect of these compounds on the ASP4058-mediated inhibition of trans-endothelial diffusion of FITC-labelled dextran was examined. Data represent mean ± SEM ($n = 6$ in F, $n = 5$ in G). * $P < 0.05$.

significant inhibition was seen at 10 nM (Figure 2E), which is a concentration that acts as an agonist without internalizing S1P₁ receptors (Figure 2B–D). This effect of ASP4058 was reversed by the addition of TASP0277308, a selective S1P₁ antagonist (Fujii *et al.*, 2012) (Figure 2F), suggesting that ASP4058 tightens the cell–cell junction of HCTAECs and promotes an endothelial barrier *via* stimulation of S1P₁ receptors. It was reported previously that Rac1 is activated in response to S1P₁ signalling and strengthens the barrier function of endothelial cells by enhancing actin cytoskeleton-mediated accumulation of barrier components in junctions between these cells (Wang and Dudek, 2009). Consistent with this report, pre-incubation with a Rac1

inhibitor, EHOp-016 (Montalvo-Ortiz *et al.*, 2012), ameliorated the effect of ASP4058 on permeability (Figure 2G).

Effect of ASP4058 on trans-endothelial migration of monocytes *in vitro*

The macrophage is a major inflammatory cell type present in human IA lesion (Chyatte *et al.*, 1999; Frosen *et al.*, 2004). Recent studies suggest that MCP-1 recruits monocytes in the peripheral blood to the lesion (Aoki *et al.*, 2009; Kanematsu *et al.*, 2011), and these cells function to drive inflammation there to develop IA (Aoki *et al.*, 2009; Aoki and Narumiya, 2012; Fukuda and Aoki, 2015). We, therefore, used a Transwell system and examined whether

Table 1

Effects of S1P receptor agonists used in this study on human S1P receptor subtypes

Compound	EC ₅₀ (nM)				
	hS1P ₁	hS1P ₂	hS1P ₃	hS1P ₄	hS1P ₅
ASP4058 ^a	7.4	>10 000	920	2300	7.5
Fingolimod-P ^b	8.2	>10 000	8.4	7.2	8.2
KRP-203-P ^c	0.28	>10 000	22 (IC ₅₀) ^e	11	3
BAF312 ^d	0.39	>10 000	>1000	750	0.98

Agonistic effect of each compound was evaluated by using GTP γ S binding assay and is shown as the EC₅₀ value, except for the agonist activity of KRP-203-P on S1P₄ receptors, which was assessed by the β -arrestin signalling assay.

^aYamamoto *et al.*, 2014

^bBrinkmann *et al.*, 2002

^cScott *et al.*, 2016

^dGergely *et al.*, 2012

^eKRP-203-P acted as an inverse agonist on the S1P₃ receptor.

Fingolimod-P, fingolimod-phosphate; KRP-203-P, KRP-203-phosphate; hS1P₁₋₅, human S1P₁₋₅ receptors.

ASP4058 could prevent the trans-endothelial migration of monocytes *in vitro*. HCtAECs were cultured in a monolayer on the Transwell insert, upon which THP-1 were loaded. Recombinant MCP-1 (100 ng·mL⁻¹) was then added to the lower compartment, and cells that migrated into the lower compartment across the monolayer were quantified by an ATP-based luminescent assay. As expected, MCP-1 significantly increased the trans-endothelial migration of THP-1 cells into the lower compartment (Figure 3A). This MCP-1-dependent increase in migrated cells was concentration-dependently inhibited by ASP4058 added simultaneously (Figure 3A). Notably, a selective S1P₁ antagonist, TASPO 277308, blocked this inhibitory effect of ASP4058 on trans-endothelial migration of THP-1 in a concentration-dependent

manner (Figure 3B), suggesting that this ASP4058 action is also through S1P₁ receptors. Since macrophages also express S1P₁ receptors and it is not clear whether the above effect of ASP4058 is due to its action on endothelial cells or macrophages, we carried out the same experiment with the Transwell without the HCtAEC monolayer. ASP4058 failed to inhibit the MCP-1-dependent migration of THP-1 under these conditions (Figure 3C), suggesting that ASP4058 prevents the transmigration of THP-1 cells mainly by acting on endothelial cells.

These results combined together suggest that ASP4058 acts on S1P₁ receptors expressed on endothelial cells as an agonist to promote endothelial barrier function and suppress trans-endothelial migration of monocytes/macrophages.

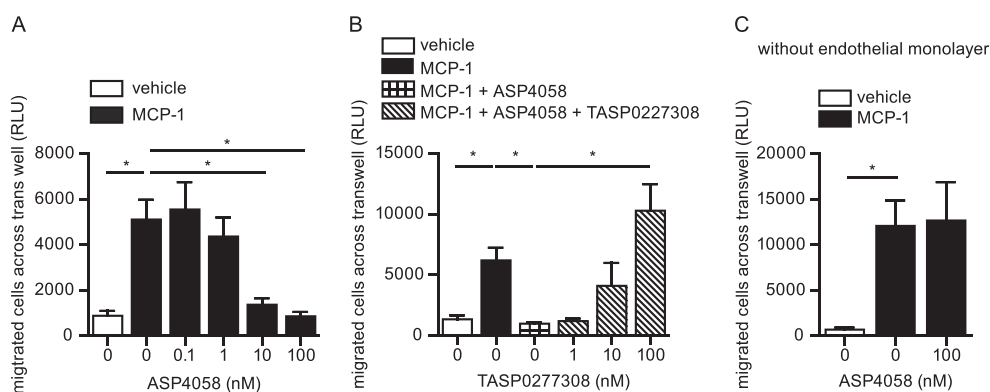


Figure 3

Inhibition of trans-endothelial migration of monocytic cells by ASP4058 mediated by the S1P₁ receptor. (A) Inhibition of MCP-1-induced trans-endothelial migration of THP-1 cells by ASP4058. Migration was measured by a Transwell assay. THP-1 cells were added into the insert well covered with HCtAEC monolayer together with the indicated concentration of ASP4058. MCP-1, 100 ng·mL⁻¹, was then added in the lower compartment and the migration of THP-1 cells across the HCtAECs was examined at 3 h by ATP-based luminescence. RLU, relative light units. Data represent mean \pm SEM ($n = 6$). * $P < 0.05$. (B) Reversal by an S1P₁ receptor antagonist TASPO277308 of the ASP4058-mediated inhibition of MCP-1-induced trans-endothelial migration of THP-1 cells. TASPO277308 was added at the indicated concentrations together with ASP4058 (100 nM) into the insert well and the lower compartment and MCP-1-induced trans-endothelial migration of THP-1 cells was examined as described in (A). Data represent mean \pm SEM ($n = 5$). * $P < 0.05$. (C) Effect of ASP4058 on MCP-1-induced chemotaxis of THP-1 cells. THP-1 cells were added to the insert well without HCtAECs in the absence or presence of 100 nM ASP4058, and the migration of THP-1 cells toward MCP-1 (10 ng·mL⁻¹) in the lower compartment for 3 h was examined by ATP-based luminescence. Data represent mean \pm SEM ($n = 5$). * $P < 0.05$.

Expression of S1P₁ receptors in endothelial cells and disrupted endothelial continuity in IA lesion of rats

The finding that ASP4058 promotes endothelial integrity via S1P₁ receptors and suppresses trans-endothelial migration of monocytes *in vitro* led us to hypothesize that pharmacological manipulation of S1P₁ receptors could be a therapeutic approach for IA. To corroborate such a hypothesis, we used rat IA models in this study. We first examined the expression of S1P₁ receptors in arterial walls at the ACA-OA bifurcation site and the IA walls induced at this bifurcation in a rat model by use of immunohistochemistry. As in the human specimens (Figure 1), S1P₁ receptors were expressed in the endothelium of IA lesions as well as in that of the prospective site of the control artery (Figure 4A). In this experiment, we also noted that endothelial continuity visualized by DyLight488-conjugated *Lycopersicon esculentum* Lectin was maintained in control arterial walls but apparently disrupted in IA walls (Figure 4A). We therefore next examined, by electron microscopy, whether IA development affects endothelial integrity *in situ*. To address this issue, we induced experimental IAs in rats, collected the affected parts of the artery on the fifth day after the induction, and subjected them to electron microscopic examination. At the prospective site of the control artery, endothelial cells were aligned continuously and there was no gap between these cells (Figure 4B). In contrast, although no loss of endothelial cells was seen in IA walls at this time point, a few endothelial cells were occasionally detached from the basement membrane, resulting in the dissociation of endothelial cell junction and gap formation (Figure 4B, arrows). Such detachment was observed in 17 out of 72 sections from 11 IA walls (number of sections from each IA wall was 4, 4, 5, 5, 5, 5, 6, 8, 10, 10 and 10), but in none of the 11 sections from the two control arteries (number of sections from each control artery was 1 and 10). Tada *et al.* (2010) reported similar inter-endothelial gap in IA walls at the early stage of the rat model. These morphological observations of disrupted endothelial integrity lead us to speculate that endothelial dysfunction may occur in some places of IA. To corroborate this and to examine whether ASP4058 can restore endothelial barrier function in injured lesions, we injected Evans blue on the seventh day after IA induction in rats and examined the trans-endothelial leakage in IA walls. The Evans blue-stained area at the ACA-OA bifurcation was significantly larger after IA induction compared with that at the prospective site of the control arteries (Figure 4C). Notably, ASP4058 dose-dependently ameliorated the increase in Evans blue leakage induced by IA induction at the bifurcation, and almost complete suppression was achieved at 0.1 mg·kg⁻¹ (Figure 4C). Our previous findings (Yamamoto *et al.*, 2014) demonstrated that the plasma concentration achieved in rats after oral administration of ASP4058 for 14 days at 0.1 mg·kg⁻¹ was 16.4 ± 0.463 ng·mL⁻¹ (equivalent to 37.1 ± 1.05 nM) at the maximum, which is higher than the EC₅₀ values of its agonistic effect on S1P₁ receptors (Table 1) but lower than the concentration sufficient to internalize S1P₁ receptors expressed on HCtAEC (Figure 2C, D). These results suggest that

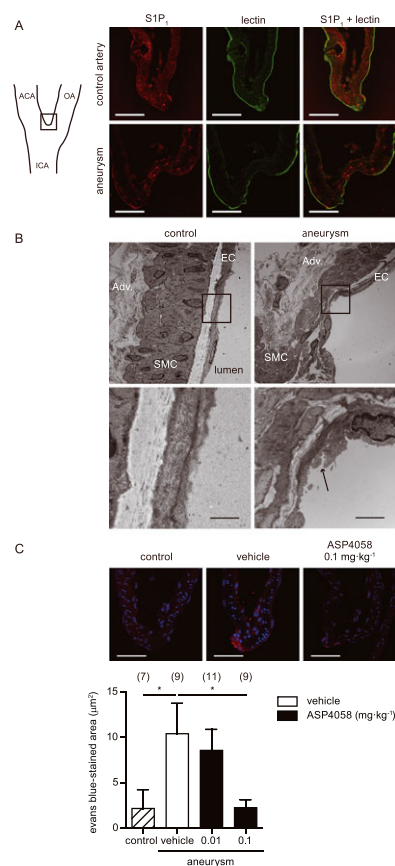


Figure 4

Expression of S1P₁ receptors in endothelial cells and disrupted endothelial continuity in the IA lesion of rats. (A) Expression of S1P₁ receptors at the ACA-OA bifurcation of control artery and the experimentally induced IA in rats. Preparations of control artery and IA at 12 weeks after its induction in rats were immunostained for S1P₁ receptors (red) and stained with DyLight488-conjugated *Lycopersicon esculentum* lectin (lectin, green) to visualize endothelial cells. Images shown are representative of 5 IA lesions. The box in the schematic drawing in the left panel indicate a region of the preparations stained. ICA, internal carotid artery. Bar, 50 µm. (B) Representative images of electron microscopic examination of control and IA wall at the ACA-OA bifurcation at the fifth day after aneurysm induction in rats. Eleven sections from two control arteries (number of sections from each control artery was 1 and 10) and 72 sections from 11 IA walls (number of sections from each IA wall was 4, 4, 5, 5, 5, 5, 6, 8, 10, 10 and 10) were examined. IA formation was facilitated by 3-aminopropionitrile treatment in these rats. Boxes in the upper panels show the region magnified in the lower panels. Note that the endothelial cells are detached at the junctions (arrows). Adv, adventitia; SMC, smooth muscle cell. Bar, 2 µm. (C) Protection by ASP4058 of IA-induced endothelial permeability in rats. IA was induced in rats and ASP4058 (0.01, 0.1 mg·kg⁻¹, once daily) was administered p.o. throughout the experimental period. Evans blue was injected i.a. on the seventh day after aneurysm induction, and the Evans blue-stained area at the ACA-OA bifurcation was evaluated as described in the Methods. Age-matched rats were used as a control. IA formation was facilitated by 3-aminopropionitrile treatment in these rats. Upper panels show the representative images of Evans blue staining (red) with nuclear staining DAPI. Bar, 50 µm. Quantitative analysis of the Evans blue-stained area is shown in the lower panel. Data represent mean ± SEM. Number of animals used is shown in parentheses. **P* < 0.05.

stimulation of S1P₁ receptor signalling can reduce the disruption of endothelial integrity in IA walls.

Effects of ASP4058 and other S1P₁ agonists on the size of IAs and macrophage infiltration in IA lesion in a rat model

We next examined whether the protective effect of ASP4058 on barrier function of IA walls could result in a reduction in the size of IAs. As the overall incidence of IAs in our rat model was 97.8% (90/92 animals examined in Figure 5A), ASP4058 did not affect the incidence. ASP4058 administered p.o. during the entire period of IA induction dose-dependently suppressed IA development, as measured by the size of the IA induced (Figure 5A), and inhibited the macrophage infiltration in the lesion at 12 weeks after the induction (Figure 5B) without significantly influencing systemic blood pressure or monocyte count in peripheral blood (Supporting Information Figure S2A, B). Consistent with the suppression of macrophage infiltration in IA walls, ASP4058 treatment almost completely suppressed the expression of MCP-1, a critical chemokine for macrophage recruitment and IA formation (Aoki *et al.*, 2009; Kanematsu *et al.*, 2011), in the IA lesion in rats (Figure 5C). The ASP4058 treatment further ameliorated the IA-associated degenerative change of the media as evidenced by the reduced thinning of smooth muscle layer (Figure 5D, Supporting Information Figure S2C).

Since ASP4058 internalizes S1P₁ receptors at high concentrations in HCtAECs (Figure 2C, D) and acts as a functional antagonist, we wondered if the suppressive actions of ASP4058 on IA can be differentiated in doses, from its actions as a functional antagonist. As a measure of the latter action, we examined the number of lymphocytes in peripheral blood. ASP4058 suppressed the lymphocyte number in peripheral blood at a dose higher than 0.03 mg·kg⁻¹ and the decrease in lymphocyte count reached a plateau at 0.1 mg·kg⁻¹ (Supporting Information Figure S2D), whereas the suppressive effect of ASP4058 on the size of the IA was observed at 0.01 mg·kg⁻¹ (Figure 5A), a dose that did not decrease the peripheral lymphocyte number (Supporting Information Figure S2D). These results suggest that the suppression of IA by ASP4058 is due to its agonistic activity, and can be achieved without affecting the lymphocyte number. The plasma concentrations of ASP4058 maintained at a dose of 0.01 mg·kg⁻¹·day⁻¹ for 12 weeks were 5.4 nM before administration, 8.8 nM at 4 h and 4.5 nM at 24 h after the administration (Table 2), and were around the EC₅₀ values examined *in vitro* (Table 1), further supporting the contribution of the agonistic action of ASP4058 to IA suppression. To experimentally corroborate this assumption, we administered a selective S1P₁ antagonist, TASP0277308, to the rat IA model twice daily at 100 or 300 mg·kg⁻¹. Although TASP0277308 potently decreased the peripheral lymphocyte count at these doses without influencing systemic blood pressure and peripheral monocyte count (Supporting Information Figure S3), it did not suppress either the macrophage infiltration in IA lesions or reduce the size of the IA (Figure 5E, F). In contrast, two structurally unrelated S1P₁ receptor-selective agonists, KRP-203 (Song *et al.*, 2008; Scott *et al.*, 2016) and BAF312 (Gergely *et al.*, 2012) (Table 1)

both significantly suppressed the growth of induced IAs without influencing systemic blood pressure (Figure 5G, Supporting Information Figure S4). We also tested the effects of the non-selective S1P agonist fingolimod (Brinkmann *et al.*, 2002) (Table 1), because this compound is the only S1P receptor agonist proven for clinical usage and is widely used as an immunosuppressant. Intriguingly, fingolimod did not suppress the size of IAs induced but, instead, significantly exacerbated the IA size without influencing systemic blood pressure (Figure 5H, Supporting Information Figure S5), suggesting the importance of selective S1P₁ receptor agonistic activity for treating IAs.

Since IAs are found as pre-existing lesions in clinical practice and the therapeutic intervention should target these pre-existing IAs, we next examined whether the administration of ASP4058 can prevent these pre-existing IAs. To this end, the administration of vehicle or ASP4058 (0.1 mg·kg⁻¹, once daily) was started 1 week after the IA induction and effects on the growth of the aneurysm were examined at 7 weeks (Figure 5I). Compared with the vehicle-treated group, ASP4058 significantly inhibited the enlargement of pre-existing aneurysm without affecting the blood pressure (Figure 5J, Supporting Information Figure S6). These findings indicate that ASP4058 has the potential to prevent the enlargement of pre-existing aneurysms, which is critical for the clinical application of ASP4058 for IA.

These results combined together suggest that ASP4058 suppresses IA by acting on S1P₁ receptors as an S1P₁ agonist.

Effect of ASP4058 on IA formation induced in non-human primates

To further explore the potential of ASP4058 for clinical use, we next examined the effect of ASP4058 on IA formation in non-human primates as an exploratory study. Because the incidence of IA is not high in this non-human primate IA model and the size of the induced IA is small, we examined the incidence of IAs in this model by measuring breakage of the lamina elastica (Supporting Information Figure S7). Female *M. fascicularis* underwent the aneurysm induction as described in the Methods and the effect of ASP4058 (0.1 mg·kg⁻¹, once daily) on IA formation at five bifurcation sites of intracranial arteries in each animal was evaluated at 52 weeks after the surgical manipulation. During this experimental period, the plasma concentration of ASP4058 was maintained high enough to stimulate S1P₁ receptors and not so high as to internalize S1P₁ receptors (Table 3). IA formation tended to be suppressed in the ASP4058-treated group compared with the vehicle-treated group ($n = 3$ in each group, five bifurcation sites per monkey (total 15 sites per group), vehicle-treated group; 11/15, ASP4058-treated group; 6/15) (Figure 5K).

Discussion

IA is a common, asymptomatic but potentially dangerous disease in the general public, which, once ruptured, leads to lethal subarachnoid haemorrhage (Wiebers *et al.*, 2002; van

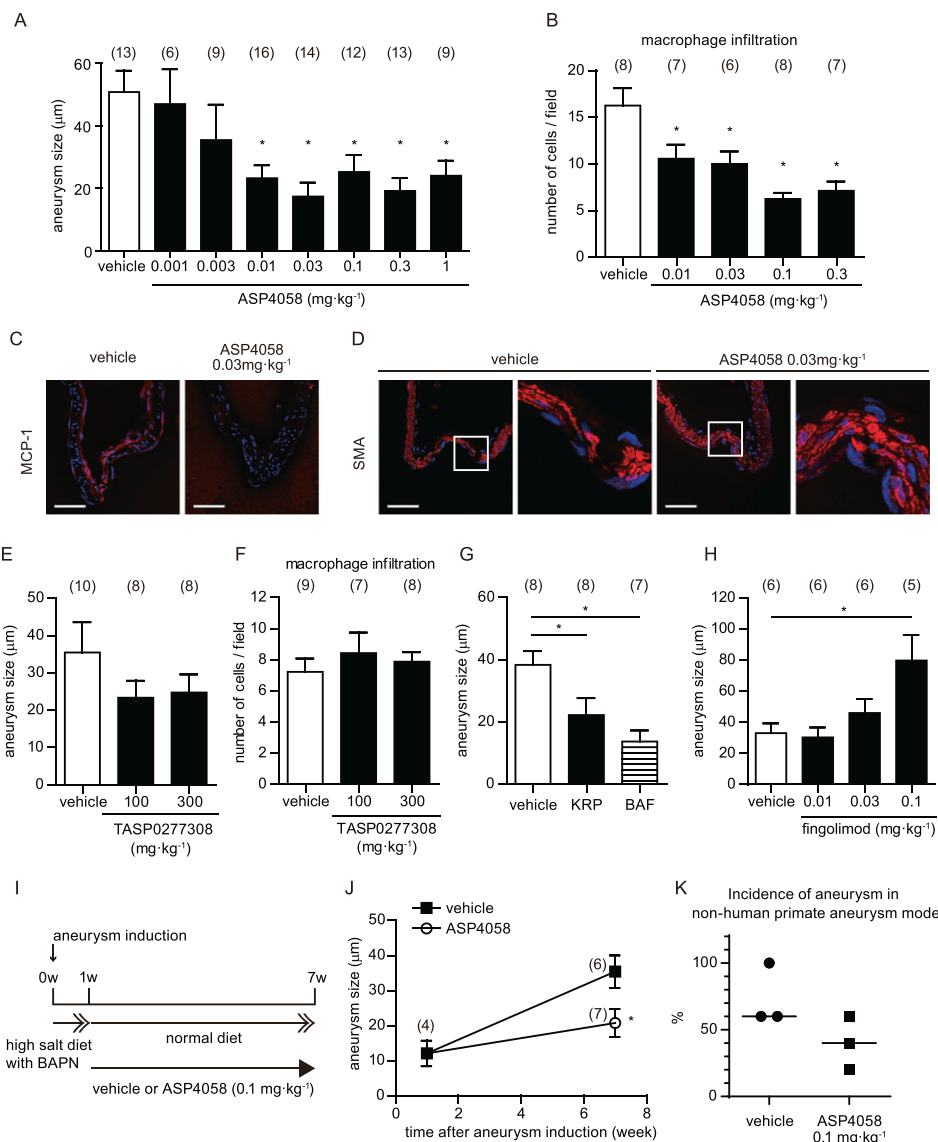


Figure 5

Suppression of IA by S1P₁ agonists in rats and non-human primates. (A, B) Concentration-dependent suppression of rat IA development by ASP4058. IA was induced in rats administered the indicated doses of ASP4058 p.o. during the whole experimental period as described in the Methods. Specimens of IA induced at the right ACA-OA bifurcation were prepared at 12 weeks after their induction, and the aneurysm size (A) and the number of macrophages infiltrated into the lesion (B) were examined. Data represent mean ± SEM. Number of animals used is shown in parentheses. (C, D) Suppression of MCP-1 expression and degenerative changes in the media in IA lesions after treatment with ASP4058. Preparations of IA lesions from vehicle or ASP4058 (0.03 mg·kg⁻¹)-treated rats were immunostained for MCP-1 (*n* = 5 per group) (C, red) and α-SMA (*n* = 12 per group) (D, red) with nuclear DAPI staining (blue). Representative images are shown. Boxes in (D) show the region magnified in the respective right panels. Bar, 50 µm. (E, F) Effect of TASP0277308, an S1P₁ antagonist, on the aneurysm size and the number of macrophages infiltrated in the lesions. IA was induced in rats administered the indicated doses of TASP0277308, p.o., twice a day during the whole experimental period. Specimens of IA induced at right ACA-OA bifurcation were prepared at 4 weeks after the induction and the aneurysm size (E) and the number of macrophages in the lesion (F) were then analysed. IA formation was facilitated by 3-aminopropionitrile treatment in these rats. Data represent mean ± SEM. Number of animals used is shown in parentheses. (G, H) Effects of S1P₁ agonists, KRP-203, BAF312 and fingolimod on the aneurysm size. KRP-203 and BAF312 were administered at 0.01 and 0.3 mg·kg⁻¹ daily (G) and fingolimod was administered daily at the indicated doses (H) during whole experimental period and the aneurysm size was examined as in (E). IA formation was facilitated by 3-aminopropionitrile treatment in these rats. Data represent mean ± SEM. Number of animals used is shown in parentheses. **P* < 0.05. (I, J) IAs were first induced in rats for 1 week, which was facilitated by 3-aminopropionitrile treatment, and then treatment with ASP4058 (0.1 mg·kg⁻¹, once a day) was started. At 7 weeks after the induction of the IA, specimens of right ACA-OA bifurcation were prepared for analysis of aneurysm size. Data represent mean ± SEM. Number of animals used is shown in parentheses. **P* < 0.05. BAPN, 3-aminopropionitrile. (K) Female *Macaca fascicularis* underwent the aneurysm induction, as described in the Methods, and the effect of ASP4058 (0.1 mg·kg⁻¹, once a day) on IA formation at five bifurcation sites of the intracranial arteries per animal was evaluated at 52 weeks after the induction. Each dot represents the incidence of aneurysm in each animal, and the horizontal bars represent the median of each group (*n* = 3 in each group).

Table 2

Plasma concentration of ASP4058 in rat aneurysm model

Dose	Dosing period	Plasma concentration (nM)					
		Pre	1 h	2 h	4 h	8 h	24 h
0.01 mg·kg ⁻¹	12 weeks	5.4 ± 0.7	6.3 ± 0.9	4.9 ± 1.6	8.8 ± 1.6	7.9 ± 1.4	4.5 ± 0.6

Rats were treated with ASP4058 (0.01 mg·kg⁻¹) for 12 weeks and then plasma was collected just before (pre) and at the indicated time points after the last administration. All values represent mean ± SEM (n = 3).

Table 3

Plasma concentration of ASP4058 in non-human primate aneurysm model

Dose	Dosing period	Plasma concentration (nM)					
		Pre	1 h	2 h	4 h	8 h	
0.1 mg·kg ⁻¹	2 weeks	7.4 ± 1.2	11 ± 3.5	15 ± 3.9	17 ± 4.2	13 ± 2.6	
	4 weeks	11 ± 2.5	14 ± 4.0	17 ± 4.7	24 ± 5.5	22 ± 3.8	
	3 months	10 ± 2.6	9.3 ± 2.2	12 ± 2.0	18 ± 1.9	19 ± 3.4	
	12 months	7.0 ± 1.0	9.4 ± 0.9	13 ± 2.1	20 ± 1.3	23 ± 1.8	

Animals were treated with ASP4058 (0.1 mg·kg⁻¹, once a day) for 2, 4 weeks, 3 or 12 months, and then plasma was collected just before (pre) and at the indicated time points after the administration in each dosing period. All values represent the mean ± SEM (n = 3).

Gijn *et al.*, 2007). Therefore, there is an urgent need to develop medical procedures to prevent the rupture of IAs. Here, we have demonstrated that S1P₁ receptor agonists, such as ASP4058, potently suppress IA and associated macrophage infiltration in animal models of IA. ASP4058 appears to exert this effect by promoting endothelial integrity. Endothelial cells are believed to be activated in response to high WSS at the site of IA, and their damage and disrupted continuity were seen in both human IA and animal models. ASP4058 enhances barrier function between endothelial cells *in vitro* as demonstrated by the concentration-dependent reduction of FITC-dextran leakage through the monolayer. Such tightening of endothelial junctions further results in the suppression of the trans-endothelial migration of macrophages. Endothelial dysfunction and macrophage infiltration are suggested as two critical mechanisms underlying IA pathology, and ASP4058 suppresses both events by acting on S1P₁ receptors in endothelial cells.

There is accumulating evidence supporting the notion that S1P-S1P₁ receptor signalling plays a crucial role in the maintenance of the physiological function of endothelial cells, especially the formation of junctions between these cells. Genetic deletion of S1P₁ receptors in mice results in premature death between E12.5 and E14.5 due to massive intraembryonic haemorrhage (Liu *et al.*, 2000), suggesting S1P₁ receptor signalling has a role in vascular permeability. Furthermore, in mice deficient in S1P₁ receptors, specifically in endothelial cells, abnormal vasculature including decreased vascularization and hyper sprouting is observed. Endothelial cell-specific deletion of S1P₁ receptors impairs the formation of the adherens junction between endothelial cells, as demonstrated by a decrease in VE-cadherin content in the trypsin digestion-resistant fraction, and enhanced FITC-dextran leakage from vessels in the retina (Jung *et al.*,

2012). This observation is consistent with our findings that stimulation of S1P₁ receptors by ASP4058 inhibited the trans-endothelial permeability both *in vitro* (Figure 2) and *in vivo* (Figure 4). Interestingly, the tightening of the adherens junction and alignment of endothelial cells in response to shear stress loading is also disturbed in S1P₁ receptor-depleted endothelial cells and HUVEC; internalization of S1P₁ receptors by FTY720-P reproduces this phenotype (Jung *et al.*, 2012). Reflecting such a role for S1P₁ receptor signalling in the tightening of the adherens junction under shear stress loading *in vitro*, abnormal vascular dilatation is present in the developing retina of endothelial cell-specific S1P₁ receptor-deficient mice. Also, decreased phosphorylation of eNOS in endothelial cells of the descending aorta in response to laminar shear stress was observed *in vivo* in these S1P₁ receptor-deficient mice (Jung *et al.*, 2012). This suggests that shear stress sensing is impaired in endothelial cell-specific S1P₁-deficient mice presumably through the malformation of adherence junction between endothelial cells. S1P₁ receptor signalling also regulates the activation of endothelial cells loaded by shear stress (Galvani *et al.*, 2015). In S1P₁ receptor activation-reporter mice in which S1P₁ receptor activation can be monitored by expression of GFP, signals for GFP are observed in the aorta of these mice especially at sites subjected to increased turbulent flow (Galvani *et al.*, 2015). Intriguingly, the protein expression of VCAM-1 and **ICAM-1** in endothelial cells is detected in the descending aorta and lesser curvature, which is augmented in mice deficient in S1P₁ receptors, specifically in endothelial cells (Galvani *et al.*, 2015). Consistently, endothelial-specific overexpression of S1P₁ receptors ameliorates expression of these molecules (Galvani *et al.*, 2015), suggesting S1P₁ receptor signalling has an inhibitory effect on the activation of endothelial cells under shear stress loading. Supporting

this notion, S1P bound to HDL, not to albumin, ameliorates the TNF- α -induced increased expression of ICAM-1 and activation of NF- κ B in HUVEC *in vitro* (Galvani *et al.*, 2015).

IA formation, enlargement and rupture are greatly influenced by haemodynamic force. IA is formed at the bifurcation sites of the intracranial artery where high WSS is loaded (Dolan *et al.*, 2013; Turjman *et al.*, 2014). In such sites, endothelial cells are activated, reflected as NF- κ B activation and the induction of VCAM-1 and COX-2. This endothelial activation is presumably in response to high WSS loaded because changes in WSS markedly alter the gene expression profile of endothelial cells (Ohura *et al.*, 2003; Aoki *et al.*, 2011). Inflammation in endothelial cells is subsequently evoked presumably through NF- κ B activation or the expression of pro-inflammatory factors, which leads to endothelial damage and weakening of endothelial integrity. Given the inhibitory role of S1P₁ receptor signalling in endothelial inflammation triggered by shear stress and S1P₁ receptor-mediated tightening of the adherens junctions between endothelial cells, activation of this signalling may counteract the machinery regulating the pathogenesis of IA. Indeed, ASP4058, by acting as an agonist on S1P₁ receptors, suppressed the size of the IAs and this was accompanied by a reduction in the trans-endothelial migration of macrophages in the lesions. This concept is pivotal as a translational research to apply experimental findings of the present study to clinical usage, because we can clearly identify the endothelial cells as a therapeutic target to effectively inhibit macrophage infiltration independently of chemoattractants present there and to suppress the resultant macrophage-evoked inflammatory responses involved in the development of IA. Once a few macrophages infiltrate in arterial walls they can form a self-amplification loop through secreting their own chemoattractant, MCP-1, in the inflammatory environment (Aoki and Narumiya, 2012; Fukuda and Aoki, 2015). Thus, targeting the endothelial barrier to prevent macrophage infiltration itself as a therapeutic strategy is presumably an effective and reasonable approach. Furthermore, because trans-endothelial migration of inflammatory or immune cells in affected sites is a common pathogenesis shared by various inflammatory diseases including atherosclerosis (Robbins *et al.*, 2013), the findings of the present study may contribute to the development of novel drug therapies for a variety of inflammatory or autoimmune diseases.

Another important point is that the compound used in this study is close to clinical application. Several adverse events such as bradycardia or pulmonary function reduction were observed in the clinical trials of fingolimod (Cohen and Chun, 2011), therefore, S1P receptor agonists have a potential risk for these adverse effect. However, our previous findings suggested that ASP4058 has a wide safety margin for these side effects, presumably due to its low activity for S1P₃ receptor, at least in preclinical models (Yamamoto *et al.*, 2014). A number of clinical trials including phase III studies for several S1P₁ agonists with low activity for the S1P₃ receptor are now ongoing, although most target autoimmune diseases such as multiple sclerosis. Therefore, a certain level of safety and excellent pharmacodynamics in humans of some of these compounds is already proved, a factor that greatly facilitates the usage of this class of drugs

for IA treatment. When applied to autoimmune diseases, S1P₁ agonists elicit their effect on lymphocytes as a functional antagonist through internalizing S1P₁ receptors and thereby promoting the retention of those lymphocyte, including auto-reactive T-cells, in lymph nodes. Therefore, the exposure level of the agonist should be maintained high enough to keep the receptor internalized continuously. However, it should be noted that the suppressive effects of ASP4058 on the IA lesion are mediated through stimulating the S1P₁ receptor as an agonist and not as a functional antagonist. Since the dose of ASP4058 capable of suppressing IA in this study is considerably lower than that used for the experimental model of multiple sclerosis, where it has an immunosuppressive effect (more than 0.1 mg·kg⁻¹) (Yamamoto *et al.*, 2014), a wider safety margin could be achieved. Moreover, we can avoid the risk of adverse events caused by its immunosuppressive effect. It should also be noted that the selectivity of compounds for the S1P₁ receptor compared to other S1P receptor subtypes is important because all the selective S1P₁ agonists tested (ASP4058, BAF312 and KRP-203) with unrelated structure show suppressive effects on the size of IA but the non-selective S1P₁ agonist, fingolimod instead exacerbates it. This may be due to the simultaneous activation of S1P₃ receptors by fingolimod because G_{12/13} activation downstream of S1P₃ receptor signalling is involved in the formation of actomyosin bundles followed by endothelial barrier disruption (Marsolais and Rosen, 2009; Spindler *et al.*, 2010). Therefore, a selective S1P₁ agonist like ASP4058 could be a strong candidate for a drug for IA treatment.

One of the major limitations of the present study is that we did not directly examine the effect of ASP4058 on the rupture of IAs because of the low incidence of spontaneous rupture in our IA model. Since most IAs are asymptomatic and only a small population of IAs rupture, it is a central question whether ASP4058 can prevent rupture. However, a recently published large observation study and meta-analysis have demonstrated that the annual rupture risk increases with the size of IAs (Morita *et al.*, 2012; Greving *et al.*, 2014). Therefore, the present findings that ASP4058 suppresses the further enlargement of pre-existing IAs may indicate that ASP4058 can serve as a drug to prevent IA rupture.

Acknowledgements

This work was supported by the Special Coordination Funds by the Ministry of Education, Culture, Sports, Science and Technology of Japan and Astellas Pharma Inc. in Creation of Innovation Centres for Advanced Interdisciplinary Research Areas. We thank K. Mizutani, S. Nakaoka, T. Ishii, T. Kurita, Y. Imai, T. Ushitani and A. Mieda for their technical assistance, and T. Ijiri, T. Arai, H. Kaimori and K. Shiota for their secretarial assistance. We also thank technical assistant from the Division of Electron Microscopic Study in Centre for Anatomical Studies at Kyoto University Graduate School of Medicine for electron microscopy, Research Centre for Animal Life Science at Shiga University

of Medicine Science and the invaluable help from neurosurgeons and secretaries at Japanese Red Cross Asahikawa Hospital.

Author contributions

R.Y., T.A., J.H., K.N., Y.H., I.A. and S.N. designed the study; R.Y., T.A., H.Ko., M.F., J.H., K.Tsu., K.Ta., Shi.N., H.M. and N.H. conducted the study; R.Y., T.A., H.Ko., M.F., J.H. analysed the data; R.Y., T.A., H.Ko., J.H., H.Ka., Y.H., I.A. and S.N. interpreted the data; R.Y. and T.A. drafted the manuscript; R.Y., T.A., H.Ko., M.F., J.H., K.Tsu., K.Ta., Shi.N., H.M., N.H., H.Ka., K.N., Y.H., I.A. and S.N. revised the content of the manuscript; R.Y., T.A., H.Ko., M.F., J.H., K.Tsu., K.Ta., Shi.N., H.M., N.H., H.Ka., K.N., Y.H., I.A. and S.N. approved the final version of the manuscript.

Conflict of interest

T.A. and S.N. are supported by the Coordination Fund from JST and Astellas Pharma Inc. R.Y., J.H., N.H., Y.H. and I.A. are employees of Astellas Pharma Inc. S.N. is a scientific advisor to Astellas Pharma Inc. R.Y., T.A., J.H., and I.A. are listed as inventors on a patent application covering the use of S1P₁ agonists described in this manuscript (Publication number: WO2014175287). No potential conflicts of interest were disclosed by the other authors.

Declaration of transparency and scientific rigour

This [Declaration](#) acknowledges that this paper adheres to the principles for transparent reporting and scientific rigour of preclinical research recommended by funding agencies, publishers and other organisations engaged with supporting research.

References

Alexander SP, Davenport AP, Kelly E, Marrion N, Peters JA, Benson HE *et al.* (2015). The concise guide to PHARMACOLOGY 2015/16: G protein-coupled receptors. *Br J Pharmacol* 172: 5744–5869.

Aoki T (2015). Inflammation mediates the pathogenesis of cerebral aneurysm and becomes therapeutic target. *Neuroimmunol Neuroinflamm* 2: 86–92.

Aoki T, Kataoka H, Ishibashi R, Nozaki K, Egashira K, Hashimoto N (2009). Impact of monocyte chemoattractant protein-1 deficiency on cerebral aneurysm formation. *Stroke* 40: 942–951.

Aoki T, Kataoka H, Shimamura M, Nakagami H, Wakayama K, Moriawaki T *et al.* (2007). NF-kappaB is a key mediator of cerebral aneurysm formation. *Circulation* 116: 2830–2840.

Aoki T, Narumiya S (2012). Prostaglandins and chronic inflammation. *Trends Pharmacol Sci* 33: 304–311.

Aoki T, Nishimura M (2010). Targeting chronic inflammation in cerebral aneurysms: focusing on NF-kappaB as a putative target of medical therapy. *Expert Opin Ther Targets* 14: 265–273.

Aoki T, Nishimura M (2011). The development and the use of experimental animal models to study the underlying mechanisms of CA formation. *J Biomed Biotechnol* 2011: 535921.

Aoki T, Nishimura M, Matsuoka T, Yamamoto K, Furuyashiki T, Kataoka H *et al.* (2011). PGE₂-EP₂ signalling in endothelium is activated by haemodynamic stress and induces cerebral aneurysm through an amplifying loop via NF-kappaB. *Br J Pharmacol* 163: 1237–1249.

Blaho VA, Hla T (2014). An update on the biology of sphingosine 1-phosphate receptors. *J Lipid Res* 55: 1596–1608.

Brinkmann V (2007). Sphingosine 1-phosphate receptors in health and disease: mechanistic insights from gene deletion studies and reverse pharmacology. *Pharmacol Ther* 115: 84–105.

Brinkmann V (2009). FTY720 (fingolimod) in multiple sclerosis: therapeutic effects in the immune and the central nervous system. *Br J Pharmacol* 158: 1173–1182.

Brinkmann V, Billich A, Baumruker T, Heining P, Schmouder R, Francis G *et al.* (2010). Fingolimod (FTY720): discovery and development of an oral drug to treat multiple sclerosis. *Nat Rev Drug Discov* 9: 883–897.

Brinkmann V, Cyster JG, Hla T (2004). FTY720: sphingosine 1-phosphate receptor-1 in the control of lymphocyte egress and endothelial barrier function. *Am J Transplant* 4: 1019–1025.

Brinkmann V, Davis MD, Heise CE, Albert R, Cottens S, Hof R *et al.* (2002). The immune modulator FTY720 targets sphingosine 1-phosphate receptors. *J Biol Chem* 277: 21453–21457.

Chyatte D, Bruno G, Desai S, Todor DR (1999). Inflammation and intracranial aneurysms. *Neurosurgery* 45: 1137–1146 discussion 1146–1137.

Cohen JA, Chun J (2011). Mechanisms of fingolimod's efficacy and adverse effects in multiple sclerosis. *Ann Neurol* 69: 759–777.

Curtis MJ, Bond RA, Spina D, Ahluwalia A, Alexander SP, Giembycz MA *et al.* (2015). Experimental design and analysis and their reporting: new guidance for publication in BJP. *Br J Pharmacol* 172: 3461–3471.

Dolan JM, Kolega J, Meng H (2013). High wall shear stress and spatial gradients in vascular pathology: a review. *Ann Biomed Eng* 41: 1411–1427.

Etminan N, Brown RD Jr, Beseoglu K, Juvela S, Raymond J, Morita A *et al.* (2015). The unruptured intracranial aneurysm treatment score: a multidisciplinary consensus. *Neurology* 85: 881–889.

Frosen J, Piippo A, Paetau A, Kangasniemi M, Niemela M, Hernesniemi J *et al.* (2004). Remodeling of saccular cerebral artery aneurysm wall is associated with rupture: histological analysis of 24 unruptured and 42 ruptured cases. *Stroke* 35: 2287–2293.

Fujii Y, Hirayama T, Ohtake H, Ono N, Inoue T, Sakurai T *et al.* (2012). Amelioration of collagen-induced arthritis by a novel S1P₁ antagonist with immunomodulatory activities. *J Immunol* 188: 206–215.

Fukuda M, Aoki T (2015). Molecular basis for intracranial aneurysm formation. *Acta Neurochir Suppl* 120: 13–15.

Galvani S, Sanson M, Blaho VA, Swendeman SL, Obinata H, Conger H *et al.* (2015). HDL-bound sphingosine 1-phosphate acts as a biased agonist for the endothelial cell receptor S1P₁ to limit vascular inflammation. *Sci Signal* 8 ra79.

- Gergely P, Nuesslein-Hildesheim B, Guerini D, Brinkmann V, Traebert M, Bruns C *et al.* (2012). The selective sphingosine 1-phosphate receptor modulator BAF312 redirects lymphocyte distribution and has species-specific effects on heart rate. *Br J Pharmacol* 167: 1035–1047.
- Greving JP, Wermer MJ, Brown RD Jr, Morita A, Juvela S, Yonekura M *et al.* (2014). Development of the PHASES score for prediction of risk of rupture of intracranial aneurysms: a pooled analysis of six prospective cohort studies. *Lancet Neurol* 13: 59–66.
- Hashimoto N, Handa H, Hazama F (1978). Experimentally induced cerebral aneurysms in rats. *Surg Neurol* 10: 3–8.
- Jamous MA, Nagahiro S, Kitazato KT, Satomi J, Satoh K (2005). Role of estrogen deficiency in the formation and progression of cerebral aneurysms. Part I: experimental study of the effect of oophorectomy in rats. *J Neurosurg* 103: 1046–1051.
- Jung B, Obinata H, Galvani S, Mendelson K, Ding BS, Skoura A *et al.* (2012). Flow-regulated endothelial S1P receptor-1 signaling sustains vascular development. *Dev Cell* 23: 600–610.
- Kanematsu Y, Kanematsu M, Kurihara C, Tada Y, Tsou TL, van Rooijen N *et al.* (2011). Critical roles of macrophages in the formation of intracranial aneurysm. *Stroke* 42: 173–178.
- Kilkenny C, Browne W, Cuthill IC, Emerson M, Altman DG (2010). Animal research: reporting *in vivo* experiments: the ARRIVE guidelines. *Br J Pharmacol* 160: 1577–1579.
- Lee JF, Zeng Q, Ozaki H, Wang L, Hand AR, Hla T *et al.* (2006). Dual roles of tight junction-associated protein, zonula occludens-1, in sphingosine 1-phosphate-mediated endothelial chemotaxis and barrier integrity. *J Biol Chem* 281: 29190–29200.
- Lee MJ, Thangada S, Claffey KP, Ancellin N, Liu CH, Kluk M *et al.* (1999). Vascular endothelial cell adherens junction assembly and morphogenesis induced by sphingosine-1-phosphate. *Cell* 99: 301–312.
- Liu CH, Thangada S, Lee MJ, Van Brocklyn JR, Spiegel S, Hla T (1999). Ligand-induced trafficking of the sphingosine-1-phosphate receptor EDG-1. *Mol Biol Cell* 10: 1179–1190.
- Liu Y, Wada R, Yamashita T, Mi Y, Deng CX, Hobson JP *et al.* (2000). Edg-1, the G protein-coupled receptor for sphingosine-1-phosphate, is essential for vascular maturation. *J Clin Invest* 106: 951–961.
- Marsolais D, Rosen H (2009). Chemical modulators of sphingosine-1-phosphate receptors as barrier-oriented therapeutic molecules. *Nat Rev Drug Discov* 8: 297–307.
- Matloubian M, Lo CG, Cinamon G, Lesneski MJ, Xu Y, Brinkmann V *et al.* (2004). Lymphocyte egress from thymus and peripheral lymphoid organs is dependent on S1P receptor 1. *Nature* 427: 355–360.
- McGrath JC, Lilley E (2015). Implementing guidelines on reporting research using animals (ARRIVE etc.): new requirements for publication in BJP. *Br J Pharmacol* 172: 3189–3193.
- Montalvo-Ortiz BL, Castillo-Pichardo L, Hernandez E, Humphries-Bickley T, De la Mota-Peynado A, Cubano LA *et al.* (2012). Characterization of EHop-016, novel small molecule inhibitor of Rac GTPase. *J Biol Chem* 287: 13228–13238.
- Morita A, Kirino T, Hashi K, Aoki N, Fukuhara S, Hashimoto N *et al.* (2012). The natural course of unruptured cerebral aneurysms in a Japanese cohort. *N Engl J Med* 366: 2474–2482.
- Ohura N, Yamamoto K, Ichioka S, Sokabe T, Nakatsuka H, Baba A *et al.* (2003). Global analysis of shear stress-responsive genes in vascular endothelial cells. *J Atheroscler Thromb* 10: 304–313.
- Robbins CS, Hilgendorf I, Weber GF, Theurl I, Iwamoto Y, Figueiredo JL *et al.* (2013). Local proliferation dominates lesional macrophage accumulation in atherosclerosis. *Nat Med* 19: 1166–1172.
- Rodrigues SF, Granger DN (2015). Blood cells and endothelial barrier function. *Tissue Barriers* 3: e978720.
- Schuchardt M, Tolle M, Prufer J, van der Giet M (2011). Pharmacological relevance and potential of sphingosine 1-phosphate in the vascular system. *Br J Pharmacol* 163: 1140–1162.
- Scott FL, Clemons B, Brooks J, Brahmachary E, Powell R, Dedman H *et al.* (2016). Ozanimod (RPC1063) is a potent sphingosine-1-phosphate receptor-1 (S1P₁) and receptor-5 (S1P₅) agonist with autoimmune disease-modifying activity. *Br J Pharmacol* 173: 1778–1792.
- Song J, Matsuda C, Kai Y, Nishida T, Nakajima K, Mizushima T *et al.* (2008). A novel sphingosine 1-phosphate receptor agonist, 2-amino-2-propanediol hydrochloride (KRP-203), regulates chronic colitis in interleukin-10 gene-deficient mice. *J Pharmacol Exp Ther* 324: 276–283.
- Southan C, Sharman JL, Benson HE, Faccenda E, Pawson AJ, Alexander SP *et al.* (2016). The IUPHAR/BPS Guide to PHARMACOLOGY in 2016: towards curated quantitative interactions between 1300 protein targets and 6000 ligands. *Nucleic Acids Res* 44: D1054–D1068.
- Spindler V, Schlegel N, Waschke J (2010). Role of GTPases in control of microvascular permeability. *Cardiovasc Res* 87: 243–253.
- Tada Y, Yagi K, Kitazato KT, Tamura T, Kinouchi T, Shimada K *et al.* (2010). Reduction of endothelial tight junction proteins is related to cerebral aneurysm formation in rats. *J Hypertens* 28: 1883–1891.
- Turjman AS, Turjman F, Edelman ER (2014). Role of fluid dynamics and inflammation in intracranial aneurysm formation. *Circulation* 129: 373–382.
- van Gijn J, Kerr RS, Rinkel GJ (2007). Subarachnoid haemorrhage. *Lancet* 369: 306–318.
- Wang L, Dudek SM (2009). Regulation of vascular permeability by sphingosine 1-phosphate. *Microvasc Res* 77: 39–45.
- Wardlaw JM, White PM (2000). The detection and management of unruptured intracranial aneurysms. *Brain* 123 (Pt 2): 205–221.
- Wiebers DO, Piepgras DG, Brown RD Jr, Meissner I, Torner J, Kassell NF *et al.* (2002). Unruptured aneurysms. *J Neurosurg* 96: 50–51 discussion 58–60.
- Xiong Y, Hla T (2014). S1P control of endothelial integrity. *Curr Top Microbiol Immunol* 378: 85–105.
- Yamamoto R, Okada Y, Hirose J, Koshika T, Kawato Y, Maeda M *et al.* (2014). ASP4058, a novel agonist for sphingosine 1-phosphate receptors 1 and 5, ameliorates rodent experimental autoimmune encephalomyelitis with a favorable safety profile. *PLoS One* 9: e110819.

Supporting Information

Additional Supporting Information may be found online in the supporting information tab for this article.

<https://doi.org/10.1111/bph.13820>

Figure S1 Specificity of anti-S1P₁ antibody used and negative control experiment of immunohistochemistry in

human specimen. (A) Increase in signal intensity by over-expression of human S1P₁ in CHO cell line. Mock (mock-CHO) or human S1P₁-over-expressed CHO cells (hS1P₁-CHO) were immunostained by anti-S1P₁ antibody. Representative images with nuclear staining DAPI are shown. Bar, 30 μm . (B) Images of immunostaining without primary antibody merged with nuclear staining DAPI are shown as a negative control. Left, middle and right images are adjacent slices of those used in Figure 1A, B and C respectively. Bar, 100 μm .

Figure S2 Effect of ASP4058 on systemic blood pressure, thickness of media and peripheral monocyte or lymphocyte count. (A) Systemic blood pressure of rats treated with each dose of ASP4058 for 12 weeks after IA induction. SBP, MBP and DBP: systolic, mean and diastolic blood pressures respectively. (B-D) Effect of ASP4058 on peripheral monocyte count (B), relative thickness of media in IA lesions (C) and peripheral lymphocyte count (D) at 12 weeks after IA induction. Thickness of media in (C) is defined as a ratio of thinnest portion in medial smooth muscle cell layer of IA walls over thickness of normal arterial walls. Data represents mean \pm SEM. Number of animals used is shown in parentheses. *, $P < 0.05$.

Figure S3 Effect of TASP0277308 on systemic blood pressure and peripheral monocyte or lymphocyte count. (A) Effect of TASP0277308 on peripheral lymphocyte count at 4 weeks after IA induction. Data represents mean \pm SEM. Number of animals used is shown in parentheses. *, $P < 0.05$. (B) Systemic blood pressure of rats treated with each dose of TASP0277308 for 4 weeks after IA induction. SBP, MBP and DBP: systolic, mean and diastolic blood pressures, respectively. Data represents mean \pm SEM. Number of animals used is shown in parentheses. (C) Effect of TASP0277308 on

peripheral monocyte count at 4 weeks after IA induction. Data represents mean \pm SEM. Number of animals used is shown in parentheses.

Figure S4 Effect of KRP-203 or BAF312 on systemic blood pressure. Systemic blood pressure of rats treated with KRP-203 (0.01 $\text{mg}\cdot\text{kg}^{-1}$) or BAF312 (0.3 $\text{mg}\cdot\text{kg}^{-1}$) for 4 weeks after IA induction. SBP, MBP and DBP: systolic, mean and diastolic blood pressures, respectively. Data represents mean \pm SEM. Number of animals used is shown in parentheses.

Figure S5 Effect of fingolimod on systemic blood pressure. Systemic blood pressure of rats treated with each dose of fingolimod for 4 weeks after IA induction. SBP, MBP and DBP: systolic, mean and diastolic blood pressures, respectively. Data represents mean \pm SEM. Number of animals used is shown in parentheses.

Figure S6 Effect of ASP4058 on systemic blood pressure. IAs were first induced in rats for 1 week and then treatment with ASP4058 (0.1 $\text{mg}\cdot\text{kg}^{-1}$) was started, as indicated in Figure 5I. At 7 weeks after the induction, systemic blood pressure of rats treated was measured as in the Methods. SBP, MBP and DBP: systolic, mean and diastolic blood pressures, respectively. Data represents mean \pm SEM. Number of animals used is shown in parentheses.

Figure S7 Aneurysm induced in non-human primate model. Female *Macaca fascicularis* was underwent the aneurysm induction as in the Methods in detail. Representative images of induced aneurysms in the non-human primate model are shown. Box in the left image indicates the region magnified in the following image. IA formation at each bifurcation was assessed after visualization of internal elastic lamina by Elastica van Gieson Staining. IA is defined as a lesion with the disrupted internal elastic lamina (arrow). Bar, 50 μm .